Bioorganic & Medicinal Chemistry 20 (2012) 6929–6939

Contents lists available at SciVerse ScienceDirect

Bioorganic & Medicinal Chemistry

journal homepage: www.elsevier.com/locate/bmc

SIB-DOTA: A trifunctional prosthetic group potentially amenable for multi-modal labeling that enhances tumor uptake of internalizing monoclonal antibodies

G. Vaidyanathan *, B. J. White, D. J. Affleck, X. G. Zhao, P. C. Welsh, D. McDougald, J. Choi, M. R. Zalutsky

Box 3808, Radiology, Duke University Medical Center, Durham, NC 27710, USA

ARTICLE INFO

Article history:
Received 9 July 2012
Revised 7 October 2012
Accepted 17 October 2012
Available online 29 October 2012

Keywords:
Monoclonal antibody
Internalization
Residualizing labels
Radioiodine

ABSTRACT

A major drawback of internalizing monoclonal antibodies (mAbs) radioiodinated with direct electrophilic approaches is that tumor retention of radioactivity is compromised by the rapid washout of iodo-tyrosine, the primary labeled catabolite for mAbs labeled via this strategy. In our continuing efforts to develop more versatile residualizing labels that could overcome this problem, we have designed SIB-DOTA, a prosthetic labeling template that combines the features of the prototypical, dehalogenation-resistant *N*-succinimidyl 3-iodobenzoate (SIB) with DOTA, a useful macrocyclic chelator for labeling with radiometals. Herein we describe the synthesis of the unlabeled standard of this prosthetic moiety, its protected tin precursor, and radioiodinated SIB-DOTA. An anti-EGFRvIII-reactive mAb, L8A4 was radiolabeled with [^{131}I]SIB-DOTA in 27.1 ± 6.2% (n = 2) conjugation yields and its targeting properties to the same mAb labeled with [^{125}I]SGMIB both in vitro and in vivo using U87MG·ΔEGFR cells and xenografts were compared. In vitro paired-label internalization assays showed that the intracellular radioactivity from [^{131}I]SIB-DOTA-L8A4 was 21.4 ± 0.5% and 26.2 ± 1.1% of initially bound radioactivity at 16 and 24 h, respectively. In comparison, these values for [^{125}I]SGMIB-L8A4 were 16.7 ± 0.5% and 14.9 ± 1.1%. Similarly, the SIB-DOTA prosthetic group provided better tumor targeting in vivo than SGMIB over 8 d period. These results suggest that SIB-DOTA warrants further evaluation as a residualizing agent for labeling internalizing mAbs including those targeted to EGFRvIII.

1. Introduction

Since the invention of hybridoma technology by Kohler and Milstein,[1] a tremendous amount of work has been done in developing monoclonal anitbodies (mAbs) in tandem with radionuclides for the radioimmunoimaging (RII) and radioimmunotherapy (RIT) of cancer.[2–4] Although there have been successful outcomes in RIT of radiation sensitive malignancies with Bexxar and Zevalin,[5,6] a serious problem with most RIT approaches is the delivery of insufficient radiation dose to tumor. While the reasons for this are multifactorial, with mAbs that undergo extensive internalization, poor retention of radioactivity is a major challenge when these mAbs are radioiodinated by the direct electrophilic approach. This is due to the rapid exocytosis of the labeled catabolite 3-iodotyrosine.[7–9]

To circumvent this problem, residualizing labels to radioiodinate internalizing mAbs have been developed, and combination of these has been shown to augment tumor radioactivity retention.[10–12] Of the several approaches that we have evaluated, two most promising ones utilize either a positively charged guanidine moiety or a short peptide consisting of charged D-amino acids in the prosthetic group.[13,14] Unlike their directly radioiodinated counterparts, insufficient tumor retention of radioactivity from radiometal-labeled mAbs is often not a problem, leading some investigators to consider radiometal-labeled mAbs as residualizing and the directly radioiodinated ones as non-residualizing.

We hypothesized that, in addition to the radiometal per se, the high hydrophilic nature of the chelating groups used for their complexation is responsible for the higher tumor retention of radioactivity seen with radiometal-labeled mAbs. The primary goal of the present work was to investigate this possibility through the synthesis and evaluation of a prosthetic group, SIB-DOTA, bearing both DOTA (2,2′,2″,2‴-(1,4,7,10-tetraazacyclododecane-1,4,7,10-tetrayl)tetraacetic acid) and iodobenzoyl moieties. This was designed by combining the structural elements of the most commonly used and versatile macrocyclic chelating group, DOTA with *N*-succinimidyl 3-iodobenzoate (SIB), the archetypal prosthetic group for dehalogenation-resistant radioiodination of mAbs and mAb fragments.[15]

Our second goal was to develop a prosthetic group that would be amenable to radiolabeling with a radiohalogen, a radiometal, or both. This characteristic makes SIB-DOTA potentially useful in

* Corresponding author. Tel.: +1 919 684 7811; fax: +1 919 684 7122.
E-mail address: ganesan.v@duke.edu (G. Vaidyanathan).

0968-0896/$ - see front matter © 2012 Elsevier Ltd. All rights reserved.
http://dx.doi.org/10.1016/j.bmc.2012.10.025

the development of theragnostic agents[16] or radiopharmaceuticals labeled with two radionuclides having different properties. Radionuclides emitting long range β-particles are more suitable for the treatment of larger tumors but are not ideal for the therapy of micrometastatic lesions. On the other hand, high linear energy transfer (LET) α-particles have shorter range in tissues and are more suitable for the treatment of smaller tumors than larger ones. To overcome this conundrum, a cocktail consisting of the same targeting vehicle individually labeled with both types of radionuclides has been proposed.[17] Using SIB-DOTA, it might be possible to radiolabel mAbs with β-emitting ^{177}Lu, and α-emitting ^{211}At, thereby providing a platform for both modes of therapy using the same molecule.

In this study, we have developed a method for the synthesis of radioiodinated SIB-DOTA and its conjugation to an anti-epidermal growth factor variant III (EGFRvIII) mAb, L8A4 that undergoes extensive internalization after receptor binding.[18] L8A4 radioiodinated using SIB-DOTA was evaluated, in comparison to the same mAb radioiodinated using *N*-succinimidyl 4-guanidinomethyl-3-iodobenzoate (SGMIB)[13]—probably the best residualizing agent that we have developed to date for radioiodination—for targeting U87ΔMG EGFRvIII-expressing cells and xenografts.

2. Results and discussion

2.1. Synthesis of standard and precursor

In order to combine the structural elements of DOTA and SIB, we sought the molecule **2**, a derivative of SIB containing an additional active ester (Scheme 1). The plan was to bridge this with DOTA employing hexane diamine, containing the universal six-carbon spacer. The bis-succinimidyl ester of 5-iodoisophthalic acid (**2**) was synthesized in two steps from the corresponding dimethyl ester. We synthesized 5-iodoisophthalic acid (**1**), a known compound,[19–24] by the hydrolysis of commercially available dimethyl ester using lithium hydroxide,[25] and converted it to the bis ester **2** by treatment with *N*-hydroxysuccinimide and EDC {*N*-Ethyl-*N*′-(3-dimethylaminopropyl)carbodiimide hydrochloride}. The DOTA derivative **6** was first functionalized with the hexane diamine by its treatment with the mono carboxybenzyl (CBZ)-protected hexane diamine under conditions reported[26] for a similar compound to render **7** (Scheme 3). The synthesis of **7** has been reported using slightly different conditions[27] and by a different method.[28] The NMR data given for this compound in these two reported studies are not quite the same. The difficulty, in general, of assignment of structures for these types of compounds from NMR data has been lamented due to the broad and overlapping nature of the peaks.[29] For this reason, we have not provided the chemical shift values; rather the actual NMR spectra of DOTA derivatives synthesized in this study are provided in the supplementary data. The low- and high-resolution mass spectral data obtained for **7** were consistent with its structure. Deprotection of CBZ group in **7** under standard conditions delivered the amine **8**[27,28,30] in almost quantitative yields. The amine **8** was coupled to the diester **2** to yield the protected standard **9**. This compound was found to be somewhat susceptible to hydrolysis under the

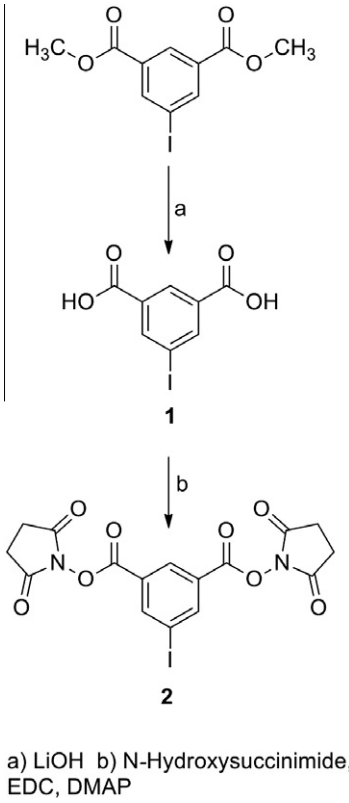

Scheme 1. Synthesis of bis-*N*-hydroxy succinimidyl 5-iodo-isophthalate.

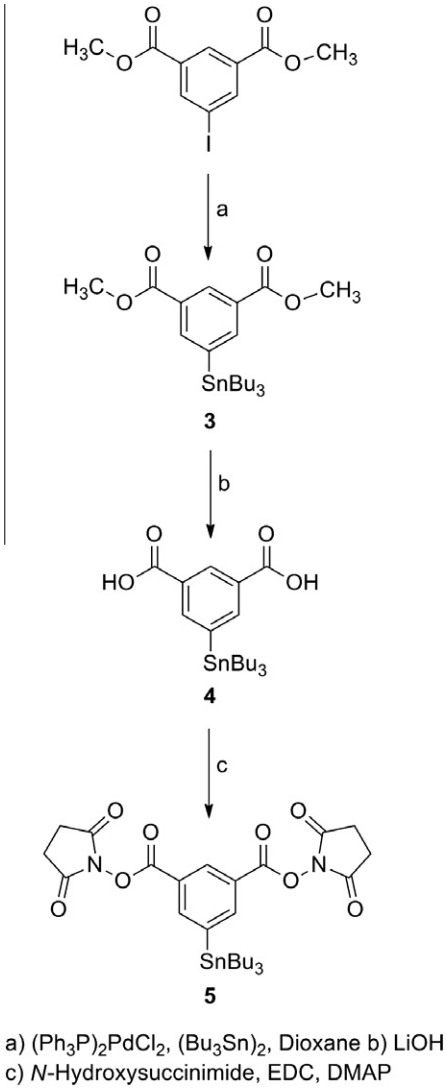

Scheme 2. Synthesis of bis-*N*-hydroxy succinimidyl 5(tri-*n*-butylstannyl) isophthalate.

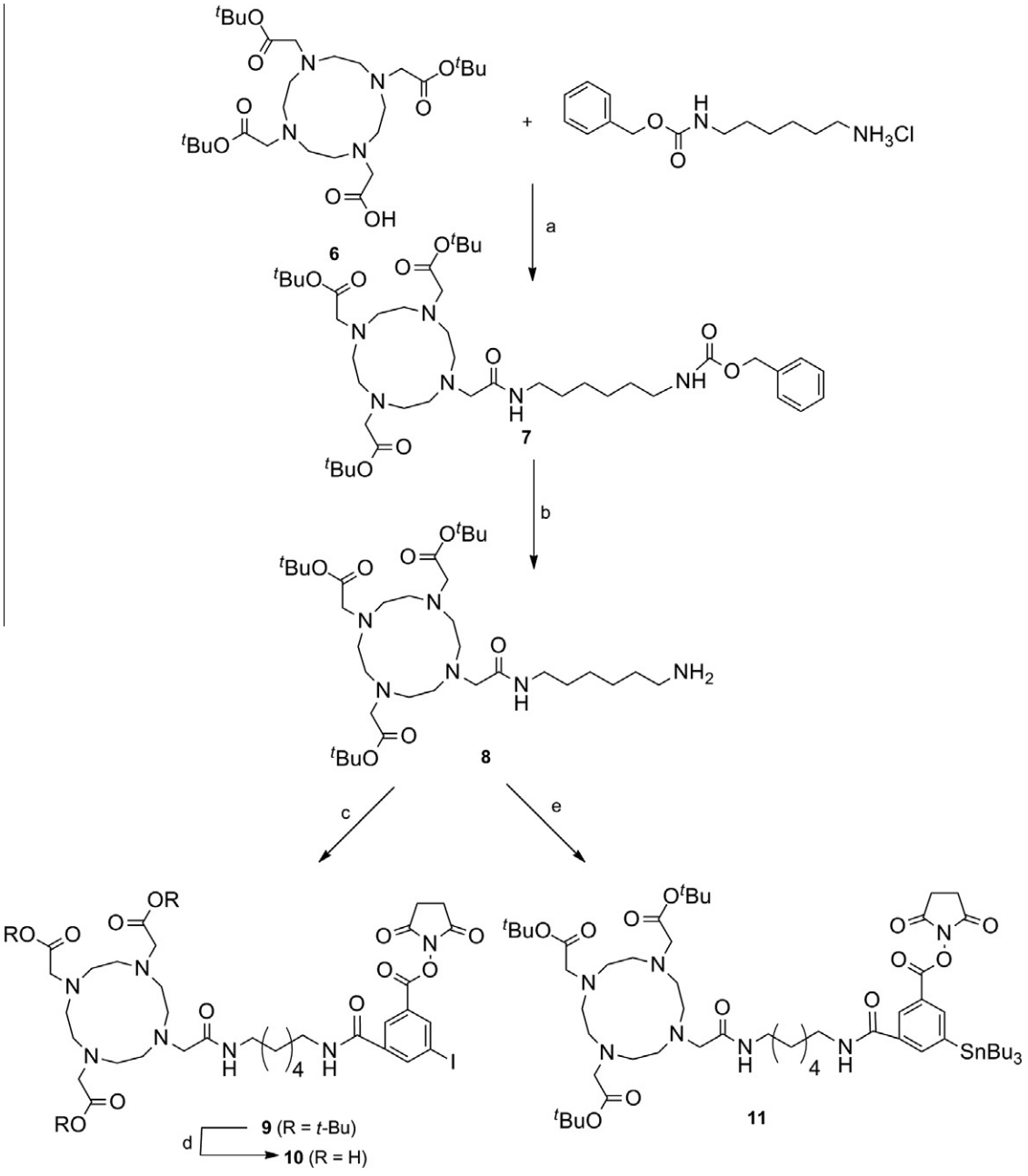

Scheme 3. Synthesis of SIB-DOTA standard and the protected tin precursor.

reversed-phase HPLC conditions used in this study. The final target compound (SIB-DOTA, **10**) was obtained by the removal of the *t*-butyl ester protecting groups in **9** by treatment with TFA; this compound also has a tendency to hydrolyze in the HPLC column.

For the synthesis of the tin precursor **11**, the di-NHS phthalate analogue (**5**) was first synthesized. For this, dimethyl 5-iodoisophthalate was stannylated under Stille conditions to obtain **3**[22] (Scheme 2). As was done with the iodo derivative, this diester was hydrolyzed to the acid **4**, and then converted to **5** by treatment with *N*-hydroxysuccinimide and EDC. Treatment of **5** with the DOTA derivative **8** resulted in the required protected tin precursor. The mass spectral data supported its identity. As with compounds **9** and **10**, this tin precursor also was somewhat labile to hydrolysis.

2.2. Radiochemistry

The tin precursor **11** was subjected to radioiodination using *N*-chlorosuccinimide (NCS) as the oxidant and acetic acid as the solvent (Scheme 4). Reversed-phase HPLC of the reaction mixture indicated the formation of some byproducts; nonetheless, radiochemical yields for the formation of [^{131}I]**9** were 85.4 ± 8.4% (n = 8). Compound [^{131}I]**9** from HPLC fractions was isolated by partitioning into ethyl acetate rather than by solid-phase extraction to minimize hydrolysis. The deprotection of the *t*-butyl groups of [^{131}I]**9** via trifluoroacetic acid (TFA) treatment was found to be very slow, needing about 2 h for complete deprotection. It should be pointed out that, although the deprotection of *t*-butyl groups from

DOTA moieties in several molecules at a macro scale has been reported to be very slow, requiring several hours,[31–36] surprisingly, the deprotection of unlabeled **9**, unlike that of its labeled analogue [^{131}I]**9**, was complete in 0.5–1 h. The isolated [^{131}I]**9** appeared homogeneous by HPLC (Fig. 1); however, there were at least two closely eluting peaks on HPLC for [^{131}I]**10**. We have not definitively identified the extra peak but speculate that it likely corresponds to the hydrolyzed product.

Conjugation of [^{131}I]**10** with mAb L8A4 was achieved in 27 ± 6% (n = 2) yields. The lower conjugation yields, compared with SIB and substituted SIB analogues,[13,37,38] might be due to partial hydrolysis of [^{131}I]**10** leaving less active ester available for conjugation. The integrity of the labeled mAb was evaluated by several methods. Size-exclusion HPLC, performed in a paired-label format by co-injecting L8A4 labeled using [^{125}I]SGMIB, indicated that, with both labeled mAbs, the radioactivity was almost completely associated with a single peak with an elution time corresponding to that of immunoglobulin (IgG) as shown in Figure 2. Paired-label trichloroacetic acid (TCA) precipitation indicated that 98.2 ± 0.1% of the radioactivity from L8A4 labeled using [^{131}I]SIB-DOTA was protein-associated compared to 99.5 ± 0.1% for [^{125}I]SGMIB-labeled mAb. Furthermore, consistent with the mild conditions used for conjugation, size-exclusion HPLC data showed no evidence of aggregate formation. From the Lindmo assay, immunoreactive fraction values of 80.7% and 82.0% were calculated for L8A4 labeled using [^{131}I]SIB-DOTA and [^{125}I]SGMIB, respectively suggesting that reaction of [^{131}I]SIB-DOTA with this mAb did not adversely affect its immunoreactivity.

2.3. Internalization of labeled mAbs

A paired-label internalization assay was performed using EGFRvIII-expressing U87MG·ΔEGFR cells to determine the effect of SIB-DOTA conjugation on the intracellular retention of radioiodine and processing of L8A4 mAb. We have found paired-label comparisons to be valuable for this purpose because previous studies have shown that while the patterns of cell processing and internalization from different studies may be similar, absolute values may vary,[13,39] possibly reflecting differences in passage and receptor number. Moreover, paired-label assays can facilitate the comparison of the relative merit of multiple labeling approaches if each paired-label experiment included one labeling method in common. In the current study, SGMIB was utilized as a benchmark not only because of its excellent residualizing properties,[13] but also because of its previous use with this cell line to evaluate the in vitro characteristics of L8A4 mAb labeled with ^{177}Lu via a variety of DOTA {and DTPA (diethylenetriaminepentaacetic acid)} ligands.[39] As shown in Figure 3A, retention of radioactivity in the intracellular compartment for [^{131}I]SIB-DOTA-L8A4 and [^{125}I]SGMIB-L8A4 were virtually identical over the first 8 h. However, beyond 8 h, intracellular radioactivity from [^{125}I]SGMIB-L8A4 plateaued, while that from the [^{131}I]SIB-DOTA-L8A4 increased steadily with the result that there was a 2-fold advantage (p = 0.003) in favor of the latter by 24 h. Differences in the amount of radioactivity present in the cell culture supernatants was complementary to that seen within the cells (Fig. 3B) and primarily reflected a larger fraction of non-protein-associated radioactivity for [^{125}I]SGMIB-L8A4. Protein-associated radioactivity in the cell culture supernatants for [^{131}I]SIB-DOTA-L8A4 ranged from 98.7 ± 1.0% at 1 h to 94.7 ± 0.0% at 24 h compared with 94.7 ± 6.0% and 79.2 ± 1.3%, respectively, for [^{125}I]SGMIB-L8A4 (Fig. 3C). These results are consistent with a higher degree of trapping of low molecular weight labeled catabolites for mAb labeled via [^{131}I]SIB-DOTA. Because SIB itself has been shown to be a poor residualizing label,[40] the characteristics of the DOTA macrocycle likely played a significant role in the enhanced intracellular

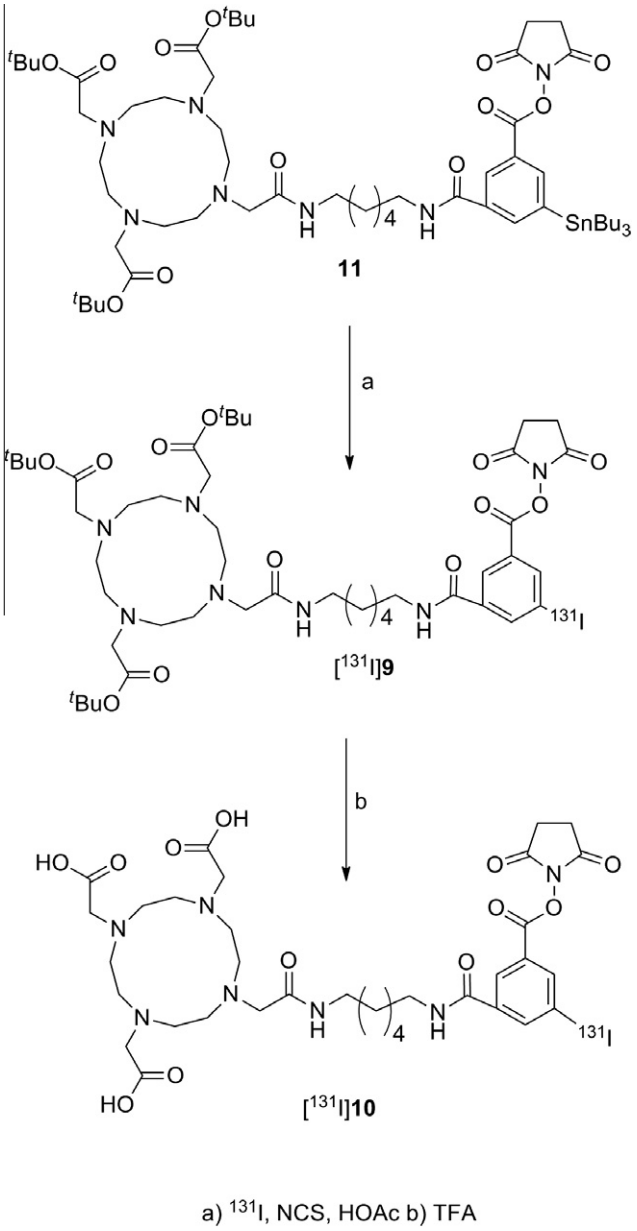

Scheme 4. Synthesis radioiodinated SIB-DOTA.

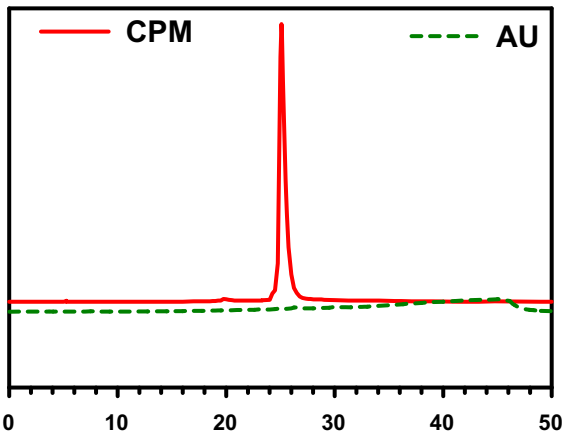

Figure 1. Reversed-phase HPLC profile of isolated [^{131}I]**9**.

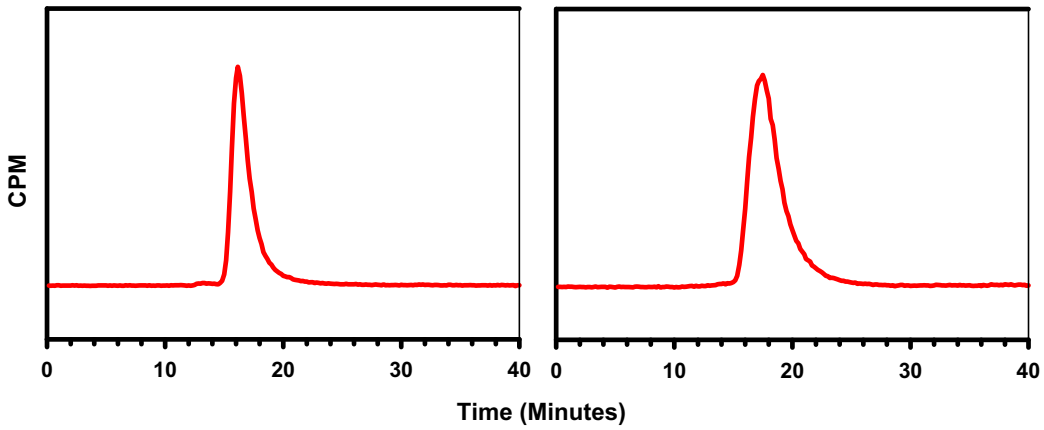

Figure 2. Radioactivity profile from the paired-label size-exclusion HPLC of [^{131}I]SIB-DOTA-L8A4 and [^{125}I]SGMIB-L8A4. Note that IgG elutes with a retention time of about 16–17 min under these conditions.

retention of radioiodine observed with mAb labeled via [^{131}I]SIB-DOTA. The increasing intracellular retention with time noted above for [^{131}I]SIB-DOTA-L8A4 has only been observed previously with one other residualizing radioiodination agent, N^{ϵ}-(3-iodobenzoyl)-Lys^5-N^{α}-maleimido-Gly^1-GEEEK (IB-Mal-D-GEEEK) that has a pentapeptide consisting of D-amino acids.[14] Although most structural characteristics of IB-Mal-D-GEEEK and SIB-DOTA are different, it is worth noting that both include 3 negatively charged COOH groups, which could impede transit of labeled catabolites across lysosomal and cell membranes. However, it is possible that the DOTA moiety could have scavenged some adventitious metals under tissue culture conditions. The net charge of the resultant macrocycle-metal complex can vary depending of the charge of the metal ion.[41] Expressing the current internalization assay results as the ratio of ^{131}I to ^{125}I activity present inside the cells facilitates comparison to results obtained with ^{177}Lu-labeled DOTA conjugates using the same mAb, cell line and [^{125}I]SGMIB-L8A4 benchmark.[39] Using the data presented in Figure 3A, ^{131}I/^{125}I ratios in U87MG·ΔEGFR cells were within error of unity from 1 through 8 h and increased to 1.28 ± 0.05 and 1.76 ± 0.15 at 16 and 24 h, respectively. These results were very similar to those obtained with L8A4 labeled with ^{177}Lu using both 2,2′,2″,2‴-(2-(4-isothiocyanatobenzyl)-1,4,7,10-tetraazacyclododecane-1,4,7,10-tetrayl) tetraacetic acid (C-DOTA) and 2, 2′,2″,2‴-(2-(1-carboxy-2-(4-isothiocyanato-2-methoxyphenyl)ethyl)-1,4,7,10-tetraazacyclododecane-1,4,7,10-tetrayl)tetraacetic acid (MeO-DOTA), where ^{177}Lu/^{125}I ratios were near unity through 8 h and then increased to 1.76 ± 0.24 and 2.09 ± 0.17, respectively, at 24 h. The observation that the intracellular retention of a radiometal and a radiohalogen are similar when associated with a DOTA conjugate is intriguing because it suggests that the superior residualizing properties of radiometal DOTA conjugates previously attributed to complex stability or transchelation to intracellular proteins may be at least partially a function of the nature of the chelating moiety.

2.4. Biodistribution in tumor-bearing mice

A paired-label tissue distribution experiment was performed in athymic mice bearing subcutaneous U87MG·ΔEGFR xenografts to evaluate the potential utility of [^{131}I]SIB-DOTA for labeling the anti-EGFRvIII mAb L8A4. As was done in the in vitro experiments, [^{125}I]SGMIB-L8A4 was co-administered as a point of reference. The uptake of radioiodine activity, expressed as a percent of injected dose per gram (%ID/g), in tumor from co-injected [^{131}I]SIB-DOTA-L8A4 and [^{125}I]SGMIB-L8A4 over a 8 d period is presented in Figure 4. At the earliest time point studied (6 h), [^{125}I]SGMIB-L8A4 exhibited slightly higher tumor uptake (15.5 ± 4.4% versus 14.0 ± 4.3%; $p = 0.002$). At subsequent time points, [^{131}I]SIB-DOTA-L8A4 had higher tumor uptake than [^{125}I]SGMIB-L8A4; however, the difference was statistically significant only at 2 d (20.6 ± 2.1% for [^{125}I]SGMIB-L8A4 versus 25.7 ± 2.1% for [^{131}I]SIB-DOTA-L8A4; $p = 0.00009$). Tumor uptake levels for [^{125}I]SGMIB-L8A4 in this xenografts model were lower than those reported previously in one study,[42] and comparable to those reported in another,[43] with this variability likely reflecting factors such as differences in EGFRvIII receptor expression and tumor size. For this reason, evaluation of the relative merit of different labeling methods was done by direct paired-label comparison and through the use of a reference labeling method—in this case, SGMIB—to compare results obtained from different experiments. In this current study, [^{131}I]SIB-DOTA-L8A4-to-[^{125}I]SGMIB-L8A4 ratios in U87MG·ΔEGFR xenografts were 1.02 ± 0.04, 1.25 ± 0.05, 1.79 ± 0.30, and 1.82 ± 0.37 at 1, 2, 6 and 8 d, respectively. The enhancement in tumor uptake observed with [^{131}I]SIB-DOTA was significantly better than that obtained with [^{177}Lu]C-DOTA-L8A4, where ^{177}Lu-to-^{125}I ratios in this xenograft were lower at most of these same time points (1.16 ± 0.14, 0.99 ± 0.33, 1.05 ± 0.78, and 1.26 ± 0.86, respectively[43]). On the other hand, the ^{177}Lu-to-^{125}I ratios measured for [^{177}Lu]-MeO-DOTA-L8A4 versus [^{125}I]SGMIB-L8A4 (1.53 ± 0.06, 2.66 ± 0.49, 5.36 ± 1.62, and 4.88 ± 2.19, respectively[43]) were higher than those determined in the current experiment for [^{131}I]SIB-DOTA. It is worth noting that the C-DOTA bifunctional chelate has a greater structural similarity to SIB-DOTA used in the current study.

The data for normal tissues are given in Table 1. Because of the proclivity of free iodide for the thyroid, uptake of radioiodine in this tissue after injection of radioiodinated mAbs can be utilized as an indicator of dehalogenation in vivo. Thyroid accumulation of mAb labeled using [^{131}I]SIB-DOTA was less than 0.5% of the injected dose (ID) at all time points and comparable to levels observed for co-administered [^{125}I]SGMIB-L8A4. These results are in agreement with those reported previously for mAbs labeled using the original SIB reagent and SGMIB.[13,44] Two tissues with notable differences in uptake for mAb labeled using [^{131}I]SIB-DOTA and [^{125}I]SGMIB were the liver and kidneys, where radioactivity levels were about 50–75% and 50–90% higher, respectively, for [^{131}I]SIB-DOTA-L8A4 between 24 and 144 h. Although L8A4 mAb has not been labeled with the original SIB reagent that lacks DOTA functionality, liver and kidney levels with other mAbs labeled via

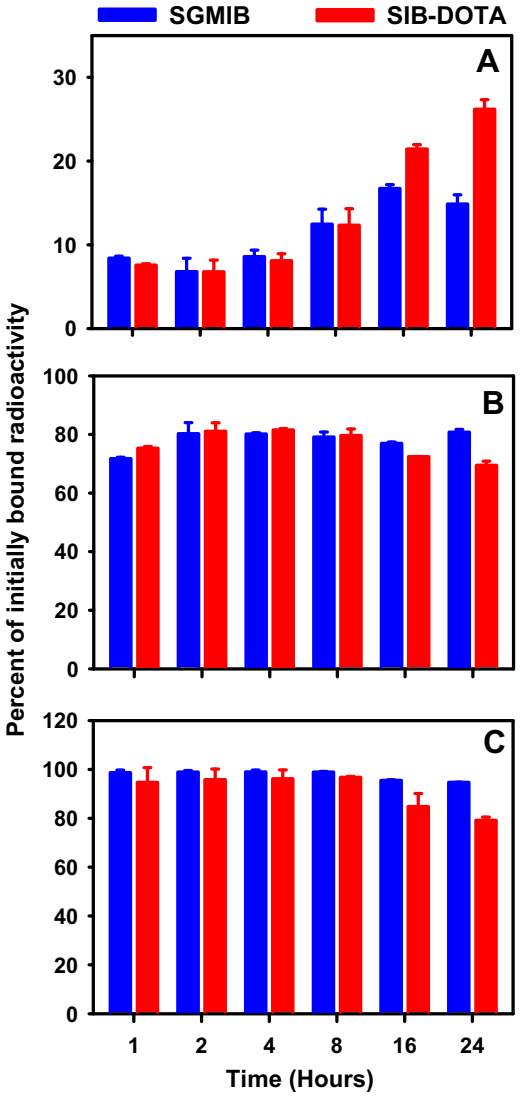

Figure 3. Results from the paired-label internalization of L8A4 labeled with [^{131}I]SIB-DOTA (red bars) and that with [^{125}I]SGMIB (blue bars) by U87MG·ΔEGFR cells. Cells were incubated with the labeled mAbs at 4 °C for 1 h, unbound radioactivity was washed, and the cells were brought up to 37 °C. Thereafter, cells were processed as described in the experimental section at various time points to determine the percent of initially bound radioactivity that was internalized (A) and that was in cell culture supernatants (B). Data in C shows the percent of radioactivity in the supernatants that could be precipitated with MeOH.

SIB are quite low,[44] suggesting that the higher liver and kidney levels observed with [^{131}I]SIB-DOTA-L8A4 may be related to the effects of the DOTA moiety. It is worth noting that with ^{177}Lu-DOTA L8A4 conjugates, liver and kidney levels were up to 500% higher than those observed for co-administered [^{125}I]SGMIB-L8A4,[43] and was about 10 times greater than that observed for the radioiodinated DOTA conjugate in the current study.

The selectivity of [^{131}I]SIB-DOTA-L8A4 targeting was evaluated by calculation of tumor-to-normal tissue ratios, the values of which for selected organs are presented in Table 2. Tumor-to-normal tissue ratios for [^{131}I]SIB-DOTA-L8A4 were higher than or comparable to those for co-administered [^{125}I]SGMIB-L8A4 at most time points in most tissues except the kidneys and the liver. Except in blood, tumor-to-normal tissue ratios for [^{131}I]SIB-DOTA-L8A4 were generally somewhat higher than those reported previously for ^{177}Lu-labeled C-DOTA-L8A4 and MeO-DOTA-L8A4.[43]

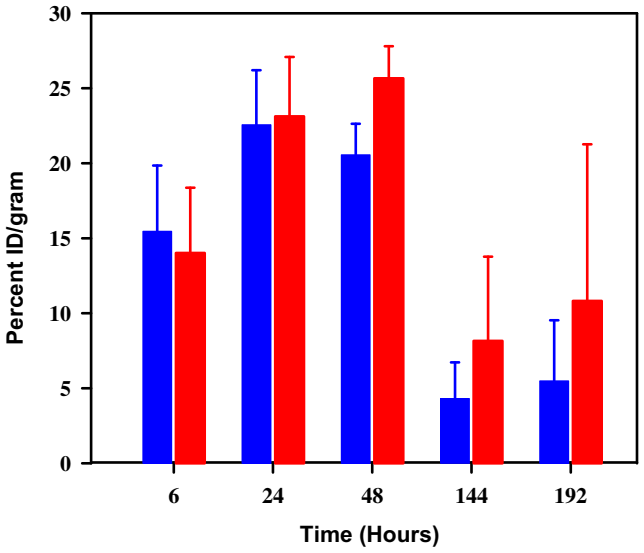

Figure 4. Tumor uptake of L8A4 labeled with [^{131}I]SIB-DOTA (red bars) and that with [^{125}I]SGMIB (blue bars) after intravenous administration in mice bearing U87MG·ΔEGFR xenografts (n = 5 per time point).

3. Conclusion

In summary, we have designed and synthesized a prosthetic group containing the structural elements of DOTA and SIB, which should allow labeling of mAbs with radiometals and radiohalogens with the same reagent. When used for radioiodination of the rapidly internalizing anti-EGFRvIII mAb L8A4, SIB-DOTA resulted in excellent trapping of radioactivity in EGFRvIII-expressing tumor cells in vitro and was effective in achieving selective targeting in human glioma xenografts expressing this mutant receptor. It appears that the highly hydrophilic DOTA moiety contributes to the higher intracellular retention of radioiodine activity. If similar results can be obtained with a radiometal such as ^{177}Lu, it might be possible to utilize SIB-DOTA for developing radioimmnuotherapeutic cocktails or theragnostic reagents labeled with radiohalogens and radiometals. For this reason, we shall evaluate the potential utility of SIB-DOTA for labeling this internalizing mAb with ^{177}Lu. Direct comparison of the internalization and in vivo tumor targeting of ^{131}I- and ^{177}Lu-labeled SIB-DOTA-L8A4 conjugates should also be interesting from a radiopharmaceutical design perspective because it could lead to a better understanding of the roles played by the radiometal and the chelate in achieving effective residualization of radioactivity in tumor cells after mAb internalization. However, one drawback of SIB-DOTA is its susceptibility to hydrolysis under reversed-phase HPLC conditions. To overcome this, we also plan to replace the *N*-hydroxysuccinimide ester with hydrolytically more stable *N*-succinimidyl carbamate moiety.[45]

4. Experimental procedures

4.1. General

All chemicals were purchased from Sigma-Aldrich unless otherwise specified. Sodium [^{125}I]iodide (2200 Ci/mmol) and sodium [^{131}I]iodide (1200 Ci/mmol) as a solution in 0.1 N NaOH were procured from Perkin Elmer Life and Analytical Sciences (Boston, MA). *N*-succinimidyl 4-guanidinomethyl-3-[^{125}I]iodobenzoate ([^{125}I]SGMIB) was synthesized following protocols reported before.[13,46] Aluminum-backed sheets (Silica gel 60 F254) were used for analytical TLC, and normal-phase column chromatography

Table 1
Uptake of iodine radioactivity in various tissues after intravenous administration of L8A4 labeled with [^{131}I]SIB-DOTA and that with [^{125}I]SGMIB in mice bearing U87MG·ΔEGFR xenografts

Tissue	%Injected dose/gram[a]							
	6 h		24 h		48 h		144 h[d]	
	SGMIB	SIB-DOTA	SGMIB	SIB-DOTA	SGMIB	SIB-DOTA	SGMIB	SIB-DOTA
Liver	6.16 ± 1.64	8.29 ± 2.21	4.41 ± 0.26	6.96 ± 0.50	3.30 ± 0.80	5.45 ± 1.58	1.14 ± 0.71	1.86 ± 0.64
Spleen	4.44 ± 1.71	5.55 ± 2.07	2.78 ± 0.57	3.48 ± 0.54[c,d]	2.26 ± 0.63	2.98 ± 0.73	0.78 ± 0.58	1.20 ± 0.56
Lung	9.20 ± 2.31	8.20 ± 2.07	6.41 ± 0.97	5.71 ± 1.22	5.30 ± 1.31	4.86 ± 1.10	1.78 ± 1.32	1.72 ± 1.32[c]
Heart	5.66 ± 1.78	5.06 ± 1.59	4.24 ± 0.72	3.86 ± 0.64	2.80 ± 0.39	2.54 ± 0.37	1.02 ± 0.70	0.88 ± 0.65
Kidney	5.64 ± 1.72	6.96 ± 2.07	3.82 ± 0.21	5.99 ± 0.48	3.09 ± 0.51	5.65 ± 1.44	1.02 ± 0.71	1.75 ± 0.52
Stomach	1.32 ± 0.49	1.26 ± 0.49	0.43 ± 0.13	0.53 ± 0.22[c]	0.55 ± 0.11	0.70 ± 0.16[c]	0.26 ± 0.16	0.30 ± 0.14[c]
Sm. Intestine	1.97 ± 0.57	2.03 ± 0.57[c]	0.98 ± 0.13	1.02 ± 0.16[c]	1.04 ± 0.14	1.18 ± 0.15	0.44 ± 0.42	0.50 ± 0.42
Lg. Intestine	1.92 ± 0.59	5.03 ± 1.45	1.01 ± 0.29	1.93 ± 0.45	0.99 ± 0.47	1.66 ± 0.85	0.38 ± 0.21	0.61 ± 0.20
Thyroid[b]	0.50 ± 0.27	0.44 ± 0.25	0.37 ± 0.13	0.32 ± 0.14[c]	0.31 ± 0.12	0.27 ± 0.10	0.17 ± 0.16	0.15 ± 0.14[c]
Muscle	1.19 ± 0.20	1.03 ± 0.18	1.23 ± 0.17	1.07 ± 0.16	0.90 ± 0.09	0.77 ± 0.10	0.37 ± 0.28	0.33 ± 0.27
Blood	20.82 ± 6.10	19.31 ± 5.64	13.75 ± 1.24	12.97 ± 1.22	10.83 ± 1.93	10.24 ± 1.80	3.65 ± 2.79	3.42 ± 2.72
Bone	1.70 ± 0.48	1.61 ± 0.46	1.58 ± 0.18	1.59 ± 0.16[c]	1.18 ± 0.35	1.17 ± 0.38[c]	0.47 ± 0.24	0.50 ± 0.29[c]
Brain	0.58 ± 0.21	0.54 ± 0.20	0.43 ± 0.05	0.40 ± 0.05	0.34 ± 0.07	0.31 ± 0.06	0.13 ± 0.11	0.12 ± 0.11

[a] Mean ± SD (n = 5).
[b] %ID/organ.
[c] Difference between the uptake of two isotopes statistically NOT significant.
[d] n = 4.

Table 2
Tumor-to-normal tissue ratios of iodine radioactivity in various tissues after intravenous administration of L8A4 labeled with [^{131}I]SIB-DOTA and that with [^{125}I]SGMIB in mice bearing U87MG·ΔEGFR xenografts

Tissue	Tumor-to-normal tissue ratio[a]				
	6 h	24 h	48 h	144 h[c]	192 h
SIB-DOTA					
Liver	1.68 ± 0.31	3.32 ± 0.40	5.06 ± 1.55	4.62 ± 1.73[b]	6.39 ± 1.59[b]
Spleen	2.63 ± 0.67	7.06 ± 1.92[c]	9.00 ± 2.05[b]	7.25 ± 1.44[b]	9.17 ± 2.47[b]
Lung	1.69 ± 0.22[b]	4.35 ± 1.88[b]	5.48 ± 1.16	5.85 ± 1.11	9.02 ± 3.38
Heart	2.81 ± 0.64[b]	6.09 ± 1.24	10.27 ± 1.71	10.71 ± 31.06[b]	12.61 ± 3.10
Kidney	2.02 ± 0.24	3.85 ± 0.43	4.75 ± 1.05	4.88 ± 1.84	6.55 ± 2.04[b]
Muscle	13.46 ± 3.16[b]	21.58 ± 1.70	33.59 ± 5.26	29.70 ± 5.49	45.98 ± 6.75
Blood	0.73 ± 0.12[b]	1.77 ± 0.13	2.56 ± 0.39	3.00 ± 0.67	3.79 ± 0.91
Brain	26.99 ± 4.85[b]	59.02 ± 11.94	83.42 ± 14.08	89.09 ± 18.98	124.36 ± 31.40
SGMIB					
Liver	2.53 ± 0.52	5.13 ± 0.87	6.55 ± 1.78	4.58 ± 0.71	6.02 ± 1.41
Spleen	3.70 ± 1.07	8.68 ± 2.22[c]	9.65 ± 2.48	7.35 ± 2.22	9.35 ± 2.83
Lung	1.67 ± 0.14	3.65 ± 1.15	4.05 ± 0.90	3.17 ± 0.87	4.37 ± 1.58
Heart	2.79 ± 0.59	5.45 ± 1.21	7.49 ± 1.49	5.17 ± 0.92	6.61 ± 2.02
Kidney	2.79 ± 0.42	5.89 ± 0.70	6.76 ± 0.99	5.25 ± 0.96	7.09 ± 1.83
Muscle	12.76 ± 2.41	18.28 ± 0.94	23.12 ± 3.28	14.75 ± 3.15	22.62 ± 4.56
Blood	0.75 ± 0.13	1.63 ± 0.14	1.93 ± 0.28	1.54 ± 0.38	1.96 ± 0.52
Brain	28.40 ± 6.26	53.62 ± 10.18	61.80 ± 10.71	43.86 ± 10.61	61.20 ± 16.97

[a] Mean ± SD (n = 5).
[b] Difference between the values for the two agents statistically NOT significant.
[c] n = 4.

was performed using silica gel 60 (both obtained from EM Science, Gibbstown, NJ). High-pressure liquid chromatography (HPLC) was performed using the following systems: (1) For analytical and semi-preparative HPLC of unlabeled compounds: a Waters Model Delta 600 semi-preparative system with a Model 600 controller and a Model 2487 dual wavelength absorbance detector; data were acquired using Millenium software. (2) For radiochemical synthesis: a Beckman Gold HPLC system equipped with a Model 126 programmable solvent module, a Model 166 NM variable wavelength detector, a Model 170 radioisotope detector and a Beckman System Gold remote interface module SS420X; data were acquired using 32 Karat® software. (3) For size-exclusion HPLC: a Beckman Gold HPLC system equipped with a Model 126 programmable solvent module, a Model 168 diode array detector, and Beckman System Gold remote interface module SS420X; data was acquired using 32 Karat® software. In this system radioactivity was detected using an IN/US γ-RAM radioactivity detector and Laura Lite® software (IN/US Systems, Tampa, FL); this system has the capability to detect two isotopes simultaneously. Reversed-phase HPLC was performed using a 4.6 × 250-mm XTerra RP18 (5 μm) column and a 19 × 150-mm XTerra RP18 (7 μm) column for analytical and semi-preparative runs, respectively. Size-exclusion HPLC was performed using a TSK-GEL G3000SW (7.5 × 600 mm; 10 μm) column (TOSOH Bioscience LLC, Montgomeryville, PA) eluted with PBS, pH 7.14 at a flow rate of 1 ml/min. Melting points were determined using either a HaakeBuchler or Fisher Johns melting point apparatus and were uncorrected. Proton NMR spectra of samples were obtained on Varian- 300 MHz (Mercury) or 400 MHz (Inova) spectrometers and carbon-13 NMR spectra were obtained using either a Varian 400 MHz (inova) or a 500 MHz (Inova) NMR spectrometer; chemical shifts are reported in δ units using the residual solvent peaks as a reference. Mass spectra were recorded using one

of the following systems: (1) Shimadzu QP2010 GC/MS system, (2) Agilent LC/MSD Trap for electrospray ionization (ESI) LC/MS, (3) Agilent LCMS-TOF with DART, a high resolution mass spectrometer used for ESI, DART and LC–MS, (4) Applied Biosystems DE-PRO Biospectrometry Workstation (MALDI–MS), and/or (5) JEOL SX-102 high-resolution mass spectrometer (FAB, and EI).

4.2. Synthesis

4.2.1. 5-Iodo-isophthalic acid (1)

Dimethyl-5-iodoisophthalate (1.35 g, 4.21 mmol, Matrix Scientific, Columbia, SC) and lithium hydroxide monohydrate (884 mg, 20.07 mmol) were taken in a mixture of 3.95 mL methanol and 0.99 mL water and the suspension was stirred vigorously at 20 °C for 3.5 h. The mixture was diluted with aqueous saturated sodium bicarbonate to a volume of 75 mL, and unreacted ester was removed by extraction with 75 mL ethyl acetate. The aqueous layer was carefully acidified with 1 M HCl to pH 2 and the resultant acid was extracted twice with 250 mL ethyl acetate. The ethyl acetate fractions were combined, dried over sodium sulfate, and the ethyl acetate was evaporated to give a white powder (965 mg, 78.4%): mp 302–303 °C ^{1}H NMR-300 MHz (CD_3OD) δ 8.55 (d, 2H), 8.60 (d, 1H). ^{13}C NMR (126 MHz, CD_3OD) δ 92.6, 129.5, 132.6, 142.2, 165.7. MS (LCMS-ESI; negative ion mode) m/z: 290.7 $(M-H)^-$; HRMS (FAB^-) Calcd for $C_8H_4IO_4$ $(M-H)^-$ 290.9154. Found 290.9141 ± 0.0000 (n = 2).

4.2.2. Bis(2,5-dioxopyrrolidin-1-yl) 5-iodoisophthalate (2)

A mixture of **1** (876 mg, 3.0 mmol), *N*-hydroxysuccinimide (1.38 g, 12.0 mmol), EDC (1.73 g, 9.0 mmol, Pierce), and DMAP (~1 mg) in anhydrous methylene chloride (15 mL) was stirred at 20 °C for 16 h under argon. The reaction mixture was concentrated to approximately 5 mL and loaded onto a silica column and the column was eluted with 50–100% ethyl acetate in hexanes. Fractions containing a compound with an R_f = 0.44 in ethyl acetate were combined, and the solvents evaporated to obtain 1.42 g of a white powder. This was further passed through a short silica plug and eluted with 50–75% ethyl acetate in hexanes to yield 1.07 g (73.3%) of a white powder: mp 207–210 °C. ^{1}H NMR-400 MHz ($CDCl_3$) δ 2.93 (br s, 8H), 8.73 (fine m, 2H), 8.83 (fine m, 1H). ^{13}C NMR (101 MHz, $CDCl_3$) δ 25.6, 94.1, 127.8, 131.3, 144.7, 159.4, 168.6. LRMS (DART) m/z: 508.9 $(M+Na)^+$; HRMS (DART) Calcd for $C_{16}H_1IN_2O_8Na$ $(M+Na)^+$ 508.9452. Found 508.9440 ± 0.0005 (n = 4).

4.2.3. Dimethyl 5-(tributylstannyl)isophthalate (3)

A mixture of dimethyl-5-iodoisophthalate (1.60 g, 5.0 mmol), hexabutylditin (5.80 g, 10 mmol), and bis(triphenylphosphine) palladium(II) dichloride (253 mg, 0.36 mmol) in 40 mL of dry dioxane was heated at reflux under argon for 1 h. The dioxane was evaporated on a rotary evaporator under aspirator vacuum, and the crude product was purified by silica gel chromatography, eluting with 0–10% ethyl acetate in hexanes to give an orange oil (2.22 g, 91.7%): ^{1}H NMR-400 MHz ($CDCl_3$) δ 0.79–0.99 (m, 9H), 1.10–1.21 (m, 6H), 1.23–1.42 (m, 6H), 1.42–1.67 (m, 6H), 3.94 (s, 6H), 8.30 (fine m, 2H, J = 17.6), 8.58 (fine m, 1H). ^{13}C NMR (126 MHz, $CDCl_3$) δ 9.8, 13.6, 27.3, 29.0, 52.3, 129.6, 130.3, 141.5, 143.5 166.9. LRMS (GCMS) m/z: cluster peaks at 427 $(M\text{-Butyl})^+$, 371 $(M\text{-2Butyl+H})^+$, 315 $(M\text{-3Butyl+2H})^+$; HRMS (FAB+) Calcd for $C_{22}H_{37}O_4{}^{120}Sn$ $(M+H)^+$ 485.1704. Found 485.1709 ± 0.0009 (n = 4).

4.2.4. 5-(Tributylstannyl)isophthalic acid (4)

A suspension of **3** (1.981 g, 4.10 mmol), lithium hydroxide monohydrate (864 mg, 20.6 mmol) in methanol (3.85 mL) and water (0.96 mL) was stirred vigorously for 3.5 h. The mixture was diluted with aqueous saturated sodium bicarbonate to a volume of 75 mL, and unreacted ester was extracted into 75 mL ethyl acetate. The aqueous solution was cooled in an ice bath, and acidified to pH 4 with the gradual addition of 1 M HCl. The resultant mixture was extracted twice with 250 mL ethyl acetate. The organic fractions were combined, dried over sodium sulfate, and ethyl acetate evaporated to yield a white powder (1.21 g, 64.7%): m.p. 207–209 °C. ^{1}H NMR-400 MHz ($CDCl_3$) δ 0.82–0.99 (m, 9H), 1.14–1.28 (m, 6H), 1.28–1.45 (m, 6H), 1.45–1.70 (m, 6H), 8.45 (fine m, 2H, J = 16.8), 8.83 (fine m, 1H). ^{13}C NMR (101 MHz, CD_3OD) δ 9.1, 12.5, 26.9, 28.7, 130.1, 130.3, 141.1, 142.8, 168.0. MS (LCMS-ESI; negative ion mode) m/z: cluster peaks at 455.0 $(M-H)^-$; HRMS (FAB^-) Calcd for $C_{20}H_{31}O_4{}^{118}Sn$ $(M-H)^-$ 453.1238. Found 453.1228 ± 0.0000 (n = 2).

4.2.5. Bis(2,5-dioxopyrrolidin-1-yl) 5-(tributylstannyl) isophthalate (5)

N-Hydroxysuccinimide (1.52 g, 10.51 mmol), EDC (1.52 g, 7.93 mmol), and DMAP (~1 mg) were added to a solution of **4** (1.20 g, 2.63 mmol) in 13 mL dry dichloromethane and the mixture was stirred overnight at 20 °C. Dichloromethane was evaporated and the residual material was subjected to silica gel chromatography with 50–75% ethyl acetate in hexanes as the eluent yielding a hazy oil (1.17 g, 44.3%): ^{1}H NMR-400 MHz ($CDCl_3$) δ 0.75–1.05 (m, 9H), 1.05–1.24 (m, 6H), 1.24–1.43 (m, 6H), 1.43–1.63 (m, 6H), 2.93 (br s, 8H), 8.47 (fine m, 2H), 8.80 (fine m, 1H). ^{13}C NMR (101 MHz, $CDCl_3$) δ 9.9, 13.6, 25.7, 27.2, 28.9, 125.2, 131.8, 143.8, 145.6, 161.2, 168.9. LRMS (FAB+) m/z: cluster peaks at 649.2 $(M+H)^+$, 593.2 $(M\text{-Butyl})^+$, 536.2 $(M\text{-2 Butyls})^+$, 480.2 $(M\text{-3 Butyls})^+$; HRMS (FAB^+) Calcd for $C_{24}H_{31}N_2O_8{}^{118}Sn$ $(M-C_4H_9+H)^+$ 593.1096. Found 593.0948 ± 0.0003 (n = 4).

4.2.6. Tri-*tert*-butyl 2,2′,2″-(10-(2-((6-(((benzyloxy)carbonyl) amino)hexyl)amino)-2-oxoethyl)-1,4,7,10-tetraazacyclododecane-1,4,7-triyl)triacetate (7)

Di-isopropylethylamine (256 mg; 1.98 mmol) and 2-(3H-[1,2,3]triazolo[4,5-b]pyridin-3-yl)-1,1,3,3-tetramethylisouronium hexafluorophosphate(V) (HATU) (464 mg, 1.22 mmol), were added to a solution of 2-(4,7,10-tris(2-(*tert*-butoxy)-2-oxoethyl)-1,4,7,10-tetraazacyclododecan-1-yl)acetic acid (**6**) (465 mg, 0.81 mmol, Macrocyclics, Dallas, Texas or ChemaTech SAS, Dijon, France) in 4 mL of dry DMF. *N*-1-carbobenzyloxy-1,6-diaminohexane·HCl (352 mg, 1.23 mmol, Bachem, Torrance, CA) was added to the resultant golden yellow solution and the homogeneous mixture was stirred at 20 °C for 15–20 h. DMF was evaporated using a rotary evaporator and a high vacuum pump. The resultant oil was dissolved in a minimum amount of acetonitrile and subjected to preparative HPLC twice. For this, the semi-preparative column was eluted at 7 mL/min with a mobile phase consisting of 0.1% TFA in both water (solvent A) and acetonitrile (solvent B); the composition was kept at 10% B for 5 min and then linearly increased to 100% B in the subsequent 30 min. The fractions containing a peak eluting with a t_R of 22 min were collected and concentrated to yield 522 mg (80%) of a pale yellow foamy solid: m.p. 89-90 °C. An aliquot was analyzed using the analytical C18 column eluted with the same gradient but with a flow rate of 1 mL/min. The t_R under these conditions was 26 min and the purity was more than 95%. See Supplementary data for ^{1}H NMR and ^{13}C NMR (both in CD_3CN). LRMS (MALDI) m/z: 750.2 $(M-t-Butyl+H)^+$, 805.9 $(M+H)^+$ (100%), 827.3 $(M+Na)^+$; (FAB^+) m/z: 805.5 $(M+H)^+$; HRMS (FAB+) calcd for $C_{42}H_{73}N_6O_9$ $(M+H)^+$ 805.5439, Found 805.5452 ± 0.0006 (n = 4). The reaction was also performed at a higher scale (2 mmol), and the product was purified by silica gel chromatography using 85:15:1 ethyl acetate:methanol:acetic acid as the eluent (R_f = 0.6 in 80:20:1 ethyl acetate:methanol:acetic acid). The resultant yellow oil was decolorized by treatment of its solution in ethyl acetate with charcoal.

4.2.7. Tri-*tert*-butyl 2,2′,2″-((10-(2-((6-aminohexyl)amino)-2-oxoethyl)-1,4,7,10-tetraazacyclododecane-1,4,7-triyl)triacetate (8)

Palladium on activated carbon (10%, 53 mg) was added to a solution of **7** (410 mg; 0.51 mmol) in 25 mL methanol in a round-bottomed flask. The flask was alternatively evacuated and purged with argon a few times, and finally the argon was replaced with hydrogen. The mixture was stirred under hydrogen (balloon) for 1–2 h, filtered over a bed of Celite, and the Celite bed with the catalyst was washed with several portions of methanol. The methanol from the filtrate was evaporated to yield 322 mg (94%) of a waxy solid: mp 79–81 °C. HPLC (conditions same as for **7**): t_R = 22.8 min. See Supplementary data for ^{1}H NMR and ^{13}C NMR (both in CD_3OD). LRMS (MALDI) *m*/*z*: 695.7, 673.7, 617.6; (FAB$^+$) *m*/*z*: 693.5 (M+Na)$^+$, 671.5 (M+H)$^+$; LCMS *m*/*z*: 671.5 (M+H)$^+$, 615.4 (M-*t*-Bu)$^+$, 559.3 (M-2 *t*-Bu)$^+$, 503.3 (M-3 *t*-Bu)$^+$; HRMS (FAB$^+$) Calcd for $C_{34}H_{67}N_6O_7$ (M+H)$^+$, 671.5072. Found 671.5072 ± 0.0015 (*n* = 4).

4.2.8. Tri-*tert*-butyl 2,2′,2″-(10-(2-((6-(3-(((2,5-dioxopyrrolidin-1-yl)oxy)carbonyl)-5-iodobenzamido)hexyl)amino)-2-oxoethyl)-1,4,7,10-tetraazacyclododecane-1,4,7-triyl)triacetate (9)

A solution of **8** (74.7 mg, 0.11 mmol) in dry THF (4 mL) was added drop wise to a solution of **2** (110 mg, 0.23 mmol) and triethylamine (34 μL) in dry THF (3 mL) and the mixture stirred at 20 °C for 3–4 h. The reaction mixture was concentrated and subjected to preparative reversed-phase HPLC. For this, the semi-preparative column was eluted at 8 mL/min with a mobile phase consisting of 0.1% TFA in both water (solvent A) and acetonitrile (solvent B); the composition was kept at 5% B for 5 min and then linearly increased to 100% B in the subsequent 30 min. The fractions containing a peak eluting with a t_R of 26.2 min were collected and concentrated to yield 80.8 mg (42%) of a resinous solid: An aliquot was analyzed using the analytical C18 column and the same gradient but with a flow rate of 1 mL/min. The t_R under these conditions was 27.6 min and the purity was about 95%. See Supplementary data for ^{1}H NMR and ^{13}C NMR (both in CD_3CN). LRMS (MALDI) *m*/*z*: 1042.9 (M+H)$^+$, 945.9 (M−NHS+H)$^+$; (FAB$^+$) *m*/*z*: 1042.4 (M+H)$^+$, 945.6 (M−NHS+H)$^+$; LCMS *m*/*z*: peak 1: 1042.5, peak 2: 945.4. HRMS (FAB$^+$) Calcd for $C_{46}H_{73}IN_7O_{12}$ 1042.4362 (M+H)$^+$. Found 1042.4360 ± 0.0035 (*n* = 4).

4.2.9. 2,2′,2″-(10-(2-((6-(3-(((2,5-Dioxopyrrolidin-1-yl)oxy)carbonyl)-5-iodobenzamido)hexyl)amino)-2-oxoethyl)-1,4,7,10-tetraazacyclododecane-1,4,7-triyl)triacetic acid (10)

Trifluoroacetic acid (0.2 ml) was added to **9** (8.6 mg, 8.3 μmol) and the mixture left at 20 °C for 1 h. TFA was evaporated with an argon stream, and the residue was triturated with ether to get 6.5 mg (86%) of a glassy solid: Analytical HPLC under conditions used for **7** gave a t_R = 20 min. See Supplementary data for ^{1}H NMR and ^{13}C NMR (both in CD_3CN). LRMS (LCMS) *m*/*z*: peak 1: 874.2 (M+H)$^+$, peak 2: 777.2 (M−NHS+H)$^+$.

4.2.10. Tri-*tert*-butyl 2,2′,2″-(10-(2-((3-((2-(3-(((2,5-dioxopyrrolidin-1-yl)oxy)carbonyl)-5-(tributylstannyl)phenyl)-2-oxoethyl)amino)propyl)amino)-2-oxoethyl)-1,4,7,10-tetraazacyclododecane-1,4,7-triyl)triacetate (11)

A solution of **5** (28 mg, 0.04 mmol) 1.0 mL of anhydrous THF was added drop wise to a solution of **8** (54 mg, 0.08 mmol) and 12 μL triethylamine in 1.0 mL anhydrous THF and the mixture was stirred at 20 °C for 2 h THF was evaporated and the residue was subjected to preparative TLC using 95:5:0.1 acetonitrile:water:HOAc as the eluent. The product was eluted from the isolated band with the same solvent. The crude product containing free *N*-hydroxysuccinimide was further purified by preparative HPLC using the following gradient consisting of 0.1% HOAc in each water (A) and acetonitrile (B) and a flow rate of 7 ml/min. The proportion of solvent B was increased linearly from 30% go 50% in 30 min and then to 100% in 5 min. This yielded compound **11** (13 mg, 26.0%) as a foamy solid. Analytical HPLC was performed by eluting the analytical C18 column at a flow rate of 1 mL/min with a mobile phase consisting of 0.1% HOAc in both water (solvent A) and acetonitrile (solvent B); the composition was linearly increased from 50% B to 100% B in 30 min. The t_R for the product under these conditions was 21.4 min and the purity was about 95%; some hydrolyzed product and *N*-hydroxysuccinimide were present. See Supplementary data for ^{1}HNMR and ^{13}CNMR (both in CD_3CN). LRMS (MALDI) *m*/*z*: cluster peaks at 1226.4 (M+Na)$^+$, 1204.6 (M)$^+$; LCMS *m*/*z*: cluster peaks at 1206.7 (M+H)$^+$. HRMS (FAB$^+$) Calcd for $C_{58}H_{100}N_7O_{12}{}^{118}Sn$ (M+H)$^+$: 1204.6452. Found 1204.6470 ± 0.0010 (*n* = 4).

4.3. Radiochemistry

4.3.0.1. 2,2′,2″-(10-(2-((6-(3-(((2,5-Dioxopyrrolidin-1-yl)oxy)carbonyl)-5-[^{131}I]iodobenzamido)hexyl)amino)-2-oxoethyl)-1,4,7,10-tetraazacyclododecane-1,4,7-triyl)triacetic acid ([^{131}I]10; [^{131}I]SIB-DOTA)

Solutions of *N*-chlorosuccinimide (30 μM; 10 μL) and **11** (2.1 mM; 10 μL) in acetic acid were added in that order to dried ^{131}I (0.5–4 mCi) in a 1/2-dram vial and the reaction was allowed to proceed at 20 °C for 10–15 min. The mixture was injected onto a reversed-phase analytical HPLC column eluted with solvents and the gradient as given for compound **7** above. The fractions encompassing the predominant peak containing [^{131}I]**9** (t_R = 25 min) were collected. While the HPLC column used here was of the same brand and dimensions as used above for unlabeled compounds, it was a different one. Also, the gradient conditions were somewhat different from those used for **9** above, with the result that the t_R value for **9** given above is slightly different from that obtained here for [^{131}I]**9**. HPLC fractions containing compound [^{131}I]**9** were extracted with ethyl acetate, and the pooled ethyl acetate extract was dried with anhydrous sodium sulfate. Ethyl acetate was evaporated with a stream of argon and the dried radioactivity was treated with 100 μL trifluoroacetic acid at 20 °C for 100 min. TFA was removed with a stream of argon, and to insure the complete removal of TFA, ethyl acetate (25 μL) was added to the residual activity and evaporated; this process was repeated a couple of times. Compound [^{131}I]**10** thus obtained was used as such for conjugation with the mAb.

4.3.1. Radioiodination of anti-EGFRvIII mAb L8A4 using [^{125}I]SGMIB and [^{131}I]SIB-DOTA

A solution of mAb L8A4[47] in 0.1 M borate buffer, pH 8.5 (121 μL; 1.24 mg/mL) was added to dried [^{125}I]SGMIB (0.8 mCi) in a 1/2-dram vial. The vial was vortexed and the mixture incubated at 20 °C for 20 min. Labeled mAb was isolated by gel filtration over a PD-10 column (GE Healthcare, Piscataway, NJ, USA) that was eluted with PBS, pH 7.14. Likewise, L8A4 was labeled with [^{131}I]SIB-DOTA by incubating about 1 mCi of [^{131}I]**10** prepared as described above with the same L8A4 solution (121 μL) used for [^{125}I]SGMIB labeling; the labeled mAb was purified by gel filtration.

4.4. In vitro studies

4.4.1. Determination of protein-associated radioactivity and immunoreactive fraction

Protein-associated radioactivity for L8A4 labeled using [^{125}I]SGMIB and [^{131}I]SIB-DOTA was determined in a paired-label format. For this, about 5 ng of each labeled mAb in 25 μL PBS in triplicate was mixed with 0.8 mL of 2% (v/v) human serum albumin

in PBS and the mixture treated with 0.1 mL of 20% (w/v) TCA, mixed thoroughly and incubated at 20 °C for 45 min. The mixture was centrifuged and the pellets and the supernatants were counted for ^{125}I and ^{131}I in a dual channel automated gamma counter (LKB 1282, Wallac, Finland), and from these counts, the percentage of total radioactivity that was in the pellets (protein-associated) was calculated for each protein. The integrity of labeled proteins was further assessed by size-exclusion HPLC by co-injecting both labeled mAbs and running the HPLC using the conditions described above. The immunoreactivity of radiolabeled L8A4 also was determined in a paired-label format. Magnetic beads coated with the extracellular domain of EGFRvIII, or to control for nonspecific binding, BSA,[48] were used for this assay. Labeled mAbs, 5 ng of each in a total of 25 μL PBS, in triplicate were added to increasing volumes (10, 20 and 40 μL) of both positive and control beads in Brij buffer (115 mM NaH_2PO_4, 0.05% BSA, 0.05% Brij-35, pH 7.2) and the volume adjusted to 125 μL with the same buffer. The mixture was incubated at 20 °C with slow shaking for 45 min, and the beads and the supernatants were separated using a magnetic separator. Both the bead pellets and supernatants were counted for ^{125}I and ^{131}I and the percentage of total radioactivity that was bound to the beads was calculated. From these, the immunoreactive fractions were determined using the method of Lindmo et al.[49] by plotting the reciprocal of the net binding (total–nonspecific) versus the reciprocal of bead concentration.

4.4.2. Paired-label internalization of L8A4 labeled using [^{125}I]SGMIB and [^{131}I]SIB-DOTA

The internalization of radioiodinated L8A4 by EGFRvIII-expressing U87MG·ΔEGFR cells was determined in a paired-label experiment. This cell line was established from U87 MG glioma cells by transfecting the cells with EGFRvIII cDNA,[50] and in cell culture this line expresses an average of 4–13 × 10^5 EGFRvIII molecules per cell.[51] Cells were grown in zinc option media (Life Technologies, Inc., Grand Island, NY) containing 10% fetal calf serum and Geneticin sulfate (600 mg/mL). Cells were plated in 6-well plates at a density of 5 × 10^5 cells/well/3 mL and incubated overnight at 37 °C, in 5% CO_2 humidified atmosphere. On the day of the experiment, the cells were incubated at 4 °C for 30 min and then both labeled (^{131}I and ^{125}I) mAbs were added to the wells in a small volume (1 μg of each per well; conditions of mAb excess). The cells were incubated with the radioactivity at 4 °C for 1 h, medium containing unbound radioactivity was removed, and the cells were washed and supplemented with fresh medium. Cells were then incubated at 37 °C and processed at 0, 1, 2, 4, 8, 16, and 24 h thereafter as given below. The cell culture supernatants were removed and the cells were washed once with fresh medium. The surface-bound radioactivity was stripped off by incubating the cells with an acidic medium (zinc option, pH 2; 1 mL) at 4 °C for 10 min. The cells were further washed with the acidic medium. Finally, the cells were solubilized by incubation with 0.5 mL of 0.5 N NaOH at 20 °C for 30 min. Aliquots of cell culture supernatants, pooled acid washes, and solubilized cell fractions were then counted for ^{125}I and ^{131}I using a dual-label program. The percentages of initially bound radioactivity that was internalized, surface-bound, and present in the cell culture supernatants were calculated. The protein-associated radioactivity in the cell culture supernatants was determined by methanol precipitation.[52]

4.5. In vivo studies

4.5.1. Paired-label biodistribution of L8A4 labeled using [^{125}I]SGMIB and [^{131}I]SIB-DOTA in athymic mice bearing U87MG·ΔEGFR xenografts

The animal studies were performed following the guidelines established by the Duke University Institutional Animal Care and Use Committee. Balb/c *nu*/*nu* mice were obtained from a closed breeding colony at the Duke University Cancer Center Isolation Facility. Xenografts were established by the subcutaneous injection of 50 μL of U87MG·ΔEGFR tumor homogenates into the flank of mice weighing 20–25 g. Biodistribution studies were initiated when the tumor reached a volume of 300–500 mm^3.

Mice were injected with 2.5 μCi each of [^{125}I]SGMIB-L8A4 (1.1 μg) and [^{131}I]SIB-DOTA-L8A4 (1.81 μg) via the tail vein. At 6 h, 1, 2, 6, and 8 d after injection, groups of five mice were killed, and tumor and tissues of interest were isolated. Blood samples were obtained by retro-orbital bleeding. Blot-dried tissues were weighed and counted along with injection standards for ^{131}I and ^{125}I in using a dual-label program in the automated gamma counter. From these data %ID/g in tumor and normal tissues were calculated. The statistical significance of differences in uptake between the two tracers for both in vitro and in vivo studies was determined via the Student paired *t*-test using the Microsoft Excel program.

Acknowledgements

This work was supported in part by Grants CA42324, NS20023, CA154291, and EB008475 from the National Institutes of Health.

Supplementary data

Supplementary data (^{1}H and ^{13}C NMR spectral data of the macrocyclic moiety-containing compounds) associated with this article can be found, in the online version, at http://dx.doi.org/10.1016/j.bmc.2012.10.025.

References and notes

1. Kohler, G.; Milstein, C. *Nature* **1975**, *256*, 495.
2. Goldsmith, S. J.; Signore, A. Q. *J. Nucl. Med. Mol. Imaging* **2010**, *54*, 574.
3. Sharkey, R. M.; Goldenberg, D. M. *Curr. Opin. Invest. Drugs* **2008**, *9*, 1302.
4. Steiner, M.; Neri, D. *Clin. Cancer Res.* **2011**, *17*, 6406.
5. Srinivasan, A.; Mukherji, S. K. *Am. J. Neuroradiol.* **2011**, *32*, 637.
6. Goldsmith, S. J. *Semin. Nucl. Med.* **2010**, *40*, 122.
7. Amano, J.; Masuyama, N.; Hirota, Y.; Tanaka, Y.; Igawa, Y.; Shiokawa, R.; Okutani, T.; Miyayama, T.; Nanami, M.; Ishigai, M. *Drug Metab. Dispos.* **2010**, *38*, 2339.
8. Vervoort, L.; Burvenich, I.; Staelens, S.; Dumolyn, C.; Waegemans, E.; Van Steenkiste, M.; Baird, S. K.; Scott, A. M.; De Vos, F. *Cancer Biother. Radiopharm.* **2010**, *25*, 193.
9. van Schaijk, F. G.; Broekema, M.; Oosterwijk, E.; van Eerd, J. E.; McBride, B. J.; Goldenberg, D. M.; Corstens, F. H.; Boerman, O. C. *J. Nucl. Med.* **2005**, *46*, 1016.
10. Kato, Y.; Vaidyanathan, G.; Kaneko, M. K.; Mishima, K.; Srivastava, N.; Chandramohan, V.; Pegram, C.; Keir, S. T.; Kuan, C. T.; Bigner, D. D.; Zalutsky, M. R. *Nucl. Med. Biol.* **2010**, *37*, 785.
11. Vaidyanathan, G.; Jestin, E.; Olafsen, T.; Wu, A. M.; Zalutsky, M. R. *Nucl. Med. Biol.* **2009**, *36*, 671.
12. Stein, R.; Govindan, S. V.; Hayes, M.; Griffiths, G. L.; Hansen, H. J.; Horak, I. D.; Goldenberg, D. M. *Clin. Cancer Res.* **2005**, *11*, 2727.
13. Vaidyanathan, G.; Affleck, D. J.; Li, J.; Welsh, P.; Zalutsky, M. R. *Bioconjugate Chem.* **2001**, *12*, 428.
14. Vaidyanathan, G.; Alston, K. L.; Bigner, D. D.; Zalutsky, M. R. *Bioconjugate Chem.* **2006**, *17*, 1085.
15. Vaidyanathan, G.; Zalutsky, M. R. *Nat. Protoc.* **2006**, *1*, 707.
16. Kelkar, S. S.; Reineke, T. M. *Bioconjugate Chem.* **1879**, *2011*, 22.
17. Mairs, R. J. *Eur. J. Cancer* **1999**, *35*, 1171.
18. Reist, C. J.; Archer, G. E.; Kurpad, S. N.; Wikstrand, C. J.; Vaidyanathan, G.; Willingham, M. C.; Moscatello, D. K.; Wong, A. J.; Bigner, D. D.; Zalutsky, M. R. *Cancer Res.* **1995**, *55*, 4375.
19. Li, L.; Zhang, S.; Zhang, X.; Zheng, G. *J. Membr. Sci.* **2007**, *289*, 258.
20. Wessendorf, F.; Hirsch, A. *Tetrahedron* **2008**, *64*, 11480.
21. Alvarez, J. C.; Garcia, J. M.; de la Campa, J. G.; de Abajo, J. *Macromol. Chem. Phys.* **1997**, *198*, 3293.
22. Cielen, E.; Tahri, A.; VerHeyen, K.; Hoornaert, G. J.; DeSchryver, F. C.; Boens, N. *J. Chem. Soc., Perkin Trans. II* **1998**, 1573.
23. Yamazaki, M.; Hagiwara, T.; Sekiguchi, M.; Sawaguchi, T.; Yano, S. *Synth. Commun.* **2008**, *38*, 553.
24. Zeng, F.; Zimmerman, S. C. *J. Am. Chem. Soc.* **1996**, *118*, 5326.
25. Boger, D. L.; Goldberg, J.; Andersson, C.-M. *J. Org. Chem.* **1999**, *64*, 2422.
26. Hovinen, J. *Chem. Biodivers.* **2006**, *3*, 296.

27. Fukukawa, K.; Rossin, R.; Hagooly, A.; Pressly, E. D.; Hunt, J. N.; Messmore, B. W.; Wooley, K. L.; Welch, M. J.; Hawker, C. J. *Biomacromolecules* **2008**, *9*, 1329.
28. Barge, A.; Tei, L.; Upadhyaya, D.; Fedeli, F.; Beltrami, L.; Stefania, R.; Aime, S.; Cravotto, G. *Org. Biomol. Chem.* **2008**, *6*, 1176.
29. Anelli, P. L.; Lattuada, L.; Lorusso, V.; Lux, G.; Morisetti, A.; Morosini, P.; Serleti, M.; Uggeri, F. *J. Med. Chem.* **2004**, *47*, 3629.
30. Stefania, R.; Tei, L.; Barge, A.; Crich, S. G.; Szabo, I.; Cabella, C.; Cravotto, G.; Aime, S. *Chem. Eur. J.* **2009**, *15*, 76.
31. Schottelius, M.; Schwaiger, M.; Wester, H. J. *Tetrahedron Lett.* **2003**, *44*, 2393.
32. Thibon, A.; Pierre, V. C. *J. Am. Chem. Soc.* **2009**, *131*, 434.
33. Rami, M.; Cecchi, A.; Montero, J. L.; Innocenti, A.; Vullo, D.; Scozzafava, A.; Winum, J. Y.; Supuran, C. T. *Chem. Med. Chem.* **2008**, *3*, 1780.
34. Mizukami, S.; Tonai, K.; Kaneko, M.; Kikuchi, K. *J. Am. Chem. Soc.* **2008**, *130*, 14376.
35. Atsumi, H.; Yoshimoto, K.; Saito, S.; Ohkuma, M.; Maeda, M.; Nagasaki, Y. *Tetrahedron Lett.* **2009**, *50*, 2177.
36. De Leon-Rodriguez, L. M.; Kovacs, Z. *Bioconjugate Chem.* **2008**, *19*, 391.
37. Vaidyanathan, G.; Zalutsky, M. R. *Bioconjugate Chem.* **1990**, *1*, 387.
38. Garg, P. K.; Archer, G. E., Jr.; Bigner, D. D.; Zalutsky, M. R. *Int. J. Radiat. Appl. Instrum. A* **1989**, *40*, 485.
39. Hens, M.; Vaidyanathan, G.; Welsh, P.; Zalutsky, M. R. *Nucl. Med. Biol.* **2009**, *36*, 117.
40. Reist, C. J.; Garg, P. K.; Alston, K. L.; Bigner, D. D.; Zalutsky, M. R. *Cancer Res.* **1996**, *56*, 4970.
41. DeNardo, S. J.; Zhong, G. R.; Salako, Q.; Li, M.; DeNardo, G. L.; Meares, C. F. *J. Nucl. Med.* **1995**, *36*, 829.
42. Vaidyanathan, G.; Affleck, D. J.; Bigner, D. D.; Zalutsky, M. R. *Nucl. Med. Biol.* **2002**, *29*, 1.
43. Hens, M.; Vaidyanathan, G.; Zhao, X. G.; Bigner, D. D.; Zalutsky, M. R. *Nucl. Med. Biol.* **2010**, *37*, 741.
44. Zalutsky, M. R.; Noska, M. A.; Colapinto, E. V.; Garg, P. K.; Bigner, D. D. *Cancer Res.* **1989**, *49*, 5543.
45. Mhidia, R.; Vallin, A.; Ollivier, N.; Blanpain, A.; Shi, G.; Christiano, R.; Johannes, L.; Melnyk, O. *Bioconjugate Chem.* **2010**, *21*, 219.
46. Vaidyanathan, G.; Zalutsky, M. R. *Nat. Protoc.* **2007**, *2*, 282.
47. Humphrey, P. A.; Wong, A. J.; Vogelstein, B.; Zalutsky, M. R.; Fuller, G. N.; Archer, G. E.; Friedman, H. S.; Kwatra, M. M.; Bigner, S. H.; Bigner, D. D. *Proc. Natl. Acad. Sci. U.S.A.* **1990**, *87*, 4207.
48. Foulon, C. F.; Reist, C. J.; Bigner, D. D.; Zalutsky, M. R. *Cancer Res.* **2000**, *60*, 4453.
49. Lindmo, T.; Boven, E.; Cuttitta, F.; Fedorko, J.; Bunn, P. A., Jr. *J. Immunol. Methods* **1984**, *72*, 77.
50. Nishikawa, R.; Ji, X. D.; Harmon, R. C.; Lazar, C. S.; Gill, G. N.; Cavenee, W. K.; Huang, H. J. *Proc. Natl. Acad. Sci. U.S.A.* **1994**, *91*, 7727.
51. Reist, C. J.; Archer, G. E.; Wikstrand, C. J.; Bigner, D. D.; Zalutsky, M. R. *Cancer Res.* **1997**, *57*, 1510.
52. Reist, C. J.; Foulon, C. F.; Alston, K.; Bigner, D. D.; Zalutsky, M. R. *Nucl. Med. Biol.* **1999**, *26*, 405.